GLOBAL CHANGE BIOLOGY
BIOENERGY

GCB Bioenergy (2016) **8**, 539–549, doi: 10.1111/gcbb.12268

Nitrous oxide emissions during establishment of eight alternative cellulosic bioenergy cropping systems in the North Central United States

LAWRENCE G. OATES[1], DAVID S. DUNCAN[1], ILYA GELFAND[2,3], NEVILLE MILLAR[2,3], G. PHILIP ROBERTSON[2,3] and RANDALL D. JACKSON[1]

[1]*DOE-Great Lakes Bioenergy Research Center & Department of Agronomy, University of Wisconsin–Madison, Madison, WI 53706, USA,* [2]*DOE-Great Lakes Bioenergy Research Center & W.K. Kellogg Biological Station, Michigan State University, Hickory Corners, MI 49060, USA,* [3]*Department of Plant, Soil and Microbial Sciences, Michigan State University, East Lansing, MI 48824, USA*

Abstract

Greenhouse gas (GHG) emissions from soils are a key sustainability metric of cropping systems. During crop establishment, disruptive land-use change is known to be a critical, but under reported period, for determining GHG emissions. We measured soil N_2O emissions and potential environmental drivers of these fluxes from a three-year establishment-phase bioenergy cropping systems experiment replicated in southcentral Wisconsin (ARL) and southwestern Michigan (KBS). Cropping systems treatments were annual monocultures (continuous corn, corn–soybean–canola rotation), perennial monocultures (switchgrass, miscanthus, and poplar), and perennial polycultures (native grass mixture, early successional community, and restored prairie) all grown using best management practices specific to the system. Cumulative three-year N_2O emissions from annuals were 142% higher than from perennials, with fertilized perennials 190% higher than unfertilized perennials. Emissions ranged from 3.1 to 19.1 kg N_2O-N ha^{-1} yr^{-1} for the annuals with continuous corn > corn–soybean–canola rotation and 1.1 to 6.3 kg N_2O-N ha^{-1} yr^{-1} for perennials. Nitrous oxide peak fluxes typically were associated with precipitation events that closely followed fertilization. Bayesian modeling of N_2O fluxes based on measured environmental factors explained 33% of variability across all systems. Models trained on single systems performed well in most monocultures (e.g., $R^2 = 0.52$ for poplar) but notably worse in polycultures (e.g., $R^2 = 0.17$ for early successional, $R^2 = 0.06$ for restored prairie), indicating that simulation models that include N_2O emissions should be parameterized specific to particular plant communities. Our results indicate that perennial bioenergy crops in their establishment phase emit less N_2O than annual crops, especially when not fertilized. These findings should be considered further alongside yield and other metrics contributing to important ecosystem services.

Keywords: Bayesian model averaging, cellulosic biofuels, corn, greenhouse gas, miscanthus, poplar, restored prairie, switchgrass

Received 16 February 2015 and accepted 30 March 2015

Introduction

Nitrous oxide (N_2O) is a potent greenhouse gas (GHG) and the main contribution to radiative forcing in the atmosphere by agriculture (Robertson *et al.*, 2000). For first generation biofuels derived from edible oils and starches, N_2O emissions from feedstock production comprise a substantial proportion of their total carbon footprint (Gelfand *et al.*, 2011). The development of second-generation biofuels derived from cellulosic materials offers the potential to substantially reduce N_2O emissions associated with feedstock production (Sanderson & Adler, 2008; Smith *et al.*, 2013). As bioenergy cropping system viability is considered, the greenhouse gas emissions of these systems will be a key component of sustainability evaluation (Reay *et al.*, 2012).

Nitrous oxide emitted from soils is primarily the product of microbially driven nitrification and denitrification. These processes are influenced by a broad range of environmental factors including temperature, oxygen availability, rates of microbial activity, and the availability of nitrogen substrates (Robertson & Groffman, 2015). The effect of these factors can depend on soil-specific properties (Henault *et al.*, 2005) including the composition of the microbial community (Cavigelli & Robertson, 2001),

Correspondence: Lawrence G. Oates, tel. 608 265 4022, fax 608 262 5217, e-mail: goates@glbrc.wisc.edu

while their relative importance may differ among cropping systems (Dechow & Freibauer, 2011). Numerous process-based models have been developed in an attempt to account for these contextual effects within a generalized framework, but they are rarely calibrated to the actively managed and harvested perennial cropping systems that have emerged as leading candidates for second-generation biofuel feedstocks (Chen *et al.*, 2008). More broadly, the dynamics governing N_2O emissions in perennial cropping systems managed for biofuel feedstock production are poorly represented in the literature (but see Nikièma *et al.*, 2011, 2012; Palmer *et al.*, 2014).

While systems based on polycultures and perennial species are anticipated to emit less N_2O than conventional agricultural cropping systems, this reduction is likely to be contingent on previous land-use and conversion methodology, phase and length of establishment, soil type, and management of inputs and production processes. Land conversion to cropping systems either through extensification or intensification of open land systems such as pasture is known to significantly increase soil organic carbon (SOC) loss (Adler *et al.*, 2007; Zenone *et al.*, 2011; Sanford *et al.*, 2012). Vegetation removal and cultivation may also affect the N cycle, especially during conversion and establishment (Bouwman *et al.*, 2010; Gelfand *et al.*, 2011; Nikièma *et al.*, 2012; Ruan & Robertson, 2013) and lead to significant nitrogen loss through leaching and gaseous emissions (Robertson *et al.*, 2012; Smith *et al.*, 2013). We must improve our understanding of N_2O emissions of likely biofuel feedstock systems to help ensure that expansion of bioenergy production generates expected societal benefits (Robertson *et al.*, 2008; Dale *et al.*, 2011, 2014).

We compared the establishment-phase N_2O emissions of annual monocultures of continuous corn and corn–soybean–canola rotations; perennial monocultures of switchgrass, miscanthus, and hybrid poplar; and perennial polycultures of early successional species, native grasses, and native prairie species. Our results cover the 2- to 4-year period following planting over which many perennial crops attain 'full capacity' biomass production (McLaughlin & Adams Kszos, 2005; Anderson-Teixeira *et al.*, 2013). Our aims were to (i) provide a direct comparison of the aggregate N_2O emissions from a broad range of feedstock production systems; (ii) characterize the effects of location and year on N_2O emissions from these cropping systems; and (iii) evaluate cropping system impacts on relationships among N_2O fluxes and environmental factors.

Materials and methods

One study site was located in southwestern Michigan at Michigan State University's W.K. Kellogg Biological Station (KBS) in Hickory Corners, MI (42°23′47″ N, 85°22′26″ W and 288 m asl), and another site was located in southcentral Wisconsin, USA, at the University of Wisconsin's Arlington Agricultural Research Station (ARL) in Arlington, WI (43°17′45″ N, 89°22′48″ W and 315 m asl). Mean annual air temperature at KBS is 9.9 °C, and annual precipitation is 1027 mm (MSCO, 2013). Soils are well-drained Kalamazoo loam (fine-loamy, mixed, semi-active, mesic Typic Hapludalfs with soil $C < 15$ g kg^{-1}, $N \leq 0.13$ g kg^{-1}) developed over glacial outwash (Crum & Collins, 1995). At ARL, mean annual temperature and precipitation are 6.9 °C and 869 mm, respectively (NWS, 2013). Soils at the site are classified as Plano silt loam (fine-silty, mixed, superactive, mesic Typic Argiudolls with soil $C > 20$ g kg^{-1}, $N \geq 0.19$ g kg^{-1}) developed over glacial till (Jokela *et al.*, 2011). Experiments at both sites were established in spring 2008 in a randomized complete block design. Ten treatments (eight cropping systems including each phase of the three-phase corn–soybean–canola rotation) were represented in five blocks of 30 × 40 m plots at each location, for a total of 100 plots. The systems under study were (i) continuous no-till corn (*Zea mays* L.); (ii) corn–soybean (*Glycine max* [L.] Merr.)–canola (*Brassica napus* L.) rotation with all 3 phases represented; (iii) monoculture switchgrass (*Panicum virgatum* L.); (iv) monoculture miscanthus (*Miscanthus x giganteus*); (v) hybrid poplar (*Populus nigra x P. maximowiczii 'NM6'*) on a 6-year coppicing rotation; (vi) a mixture of five native grass species; (vii) a mixture of 18 native prairie species; and (viii) an early successional community defined by the pre-existing seed bank and novel recruitment with no management other than fertilizer application and harvest. Of note, miscanthus at ARL suffered >95% mortality over the 2008–2009 winter and was subsequently replanted in May 2010. With the exception of miscanthus at KBS and the early successional community at both sites, perennial systems did not receive N fertilizer in 2009, while poplar at both sites received N fertilizer in 2010 only (full crop and management details are given in Table S1).

Estimating nitrous oxide emissions

When soils were consistently >0 °C, N_2O fluxes were measured biweekly with additional sampling to characterize episodic events (i.e., fertilizer application and precipitation events) using vented static chambers. All measurements were made between 1000 and 1600 h local time. Cylindrical chamber bases of 28.5 cm diameter were inserted ~5 cm below the soil surface. With the chamber lid installed, the chamber had an effective headspace volume of ~10 l (~17 cm height). Lids had a septum for gas extraction and a 2-mm diameter vent and vent tube to allow for chamber pressure equilibration. Headspace gas from within the chambers was extracted immediately following lid placement with a 30-ml nylon syringe and a 23-gauge needle. Three subsequent extractions were made at 20-min intervals over a 60-min period. Glass 5.9-ml Exetainer vials (Labco Limited, Buckinghamshire, UK) were flushed with 20 ml of extracted sample and then overpressurized with 10 ml of sample to avoid contamination and facilitate analysis. At each sampling event, field standards (1 ppm N_2O, 1 ppm CH_4, and 400 ppm CO_2) and ambient air were loaded into vials to assess

potential sample loss prior to analysis. Sample CO_2, N_2O, and CH_4 concentrations were determined by gas chromatography using an infrared gas analyzer (IRGA, LiCor 820, Lincoln, NE, USA) for CO_2, an electron capture detector (micro-ECD, Agilent 7890A GC System, Santa Clara, CA, USA) for N_2O, and a flame ionization detector (FID, Agilent 7890A) for CH_4.

Visual inspection of CO_2 accumulation curves identified samples with lost pressure or other measurement problems, for which fluxes were discarded (~2% of total measured fluxes). Remaining fluxes were analyzed with the HMR package (v0.3.1, Pedersen, 2011) in the R statistical environment (v3.0.3, R Core Team, 2014) to fit gas concentrations against time with a nonlinear model (Hutchinson & Mosier, 1981), a linear regression, and a null flux based on root mean squared error minimization. Of the 4139 flux estimates, a nonlinear model was used for the 691 (16.7%) fluxes where the 95% confidence interval for the nonlinear estimate excluded the corresponding linear estimate. In all other cases, including the case of a null flux, the linear flux estimate was used. This estimate was used to calculate the aggregate flux for the day it was sampled (daily flux) by assuming the estimate was the average flux during that day. Annual fluxes were calculated by integrating the linear interpolation of daily fluxes over one calendar year (Smith & Dobbie, 2001). Cumulative three-year emissions were then calculated for each experimental plot by summing the aggregated annual emissions from the three study years within a plot.

Assessing soil environmental variables

Concurrent with trace gas sampling, soil volumetric water content (VWC) ($m^3\ m^{-3}$) and soil temperature (°C) were measured within 1 m of the chamber with a time domain reflectometer using 20-cm rods (FieldScout 300, Spectrum Technologies, Inc., Plainfield, IL, USA) and a 15-cm soil temperature probe (Checktemp 1C, Hanna Instruments, Smithfield, RI, USA), respectively. For analysis, VWC was converted to proportion of water-filled pore space (WFPS) using the equation:

$$\mathrm{WFPS} = \frac{\theta}{TP} \tag{1}$$

where θ is equal to VWC, and TP is total porosity ($m^3\ m^{-3}$) calculated using the equation:

$$TP = \left(1 - \frac{Bd}{Pd}\right) \times 100\% \tag{2}$$

where Bd is the bulk density at each site ($g\ cm^{-3}$) and Pd is particle density, assumed to be 2.65 $g\ cm^{-3}$ for both sites. Castellano *et al*. (2010) found WFPS was of limited utility as a predictor of N_2O flux across soils with differing textures. Accordingly, we scaled and centered WFPS at each site to create a new variable ($WFPS_C$) for use in analyses.

In 2009, inorganic soil nitrogen was estimated using ion resin strips (General Electric, Watertown, MA, USA) placed in the field for 1-month periods from March to November. Matched pairs of anion and cation strips were placed at each of three persistent sampling stations per plot. Each month, all six strips in each plot were collected from the field, cleaned with deionized water to remove visible soil and then extracted in 2 M KCl. Extracted strips were regenerated with 0.5 M HCl and 0.5 M $NaHCO_3$ prior to next use. For the years 2010 and 2011, soil cores to 15 cm depth were taken concurrently with N_2O measurements to estimate soil inorganic nitrogen (N) pools. A 10 g wet-weight subsample was weighed out for immediate inorganic N extraction in 2 M KCl following Robertson *et al*. (1999). Potassium chloride extracts were stored in 20-mL polyethylene scintillation vials frozen at −20 °C prior to analysis. Colorimetric determination of extracts for ammonium (NH_4^+) (USEPA method-Pub# 27200110) and nitrate (NO_3^-) (USEPA method-Pub# 27190110) was performed on a Flow Solution 3100 segmented flow injection analyzer (OI Analytical, College Station, TX, USA).

Data analysis

Emissions were analyzed with linear mixed-effect models using the NLME package (v3.1, Pinheiro *et al*., 2013) in the R statistical environment (v3.1.1, R Core Team, 2014). Nitrous oxide emissions were summed over three calendar years; sums were log-transformed prior to analysis to approximate normally distributed data. Models were constructed to analyze response variables as a function of the fixed effects of treatment (*cropping system*) and *site*, accounting for the random effect of *block* nested within site (*site/block)*. Models were improved by allowing for distinct variances among *cropping systems*, *sites*, or both, and evaluated with likelihood ratio tests. With the variance structure in place, significant fixed effects and interactions were determined by sequentially collapsing treatment levels and comparing subsequent models with likelihood ratio tests. This process continued iteratively until none of the remaining groups could be collapsed. Annual emissions considered *year* as an additional potential component of the variance structure and used *crop* rather than *cropping system* as a factor and each combination of *year* and *site* was analyzed separately. Variance structure optimization and assessment of treatment differences were conducted as described above.

Bayesian model averaging (BMA) was used to evaluate relationships between measured environmental variables and daily N_2O fluxes for *cropping system* level (Hoeting *et al*., 1999; Maroja *et al*., 2009). We conducted the model averaging process using the bic.glm function of the R package BMA (v 3.16.2.2, Raftery *et al*., 2013). Because N_2O fluxes are seldom normally distributed, and negative fluxes are biologically relevant (Schlesinger, 2013), we used a hyperbolic arcsine transformation (Burbidge *et al*., 2013) on daily flux data prior to analysis. The maximal model was defined as soil temperature, $WFPS_C$, $NO_3^-NH_4^+$, *year*, and *site*, as well as all second-order interactions among these terms. Because we used a different method for estimating inorganic N in 2009, we only used 2010 and 2011 data. Of the 2657 data points in these two years, 2176 (82%) included all environmental measures. Annual emissions recalculated from this subset were highly correlated to those obtained from the full dataset ($R^2 = 0.90$), although the range of values was slightly greater. We trained the model on the full dataset and also subsets of the data by cropping system to generate system-specific models. We then used environmental data from the full dataset to evaluate the capacity of models trained

from a given system to predict emissions from other systems or from the full dataset.

Statistical analyses are discussed in greater detail in Appendix S1.

Results

Cumulative nitrous oxide emissions over the 3-year establishment phase

Cropping systems at the Wisconsin research station (ARL) emitted 23% more N_2O than their Michigan (KBS) counterparts. The only systems for which this pattern did not hold were continuous corn and miscanthus, where emissions were not significantly different between the sites, and the native grasses, where KBS had higher cumulative emissions (Fig. 1). Note that while we did not have miscanthus data from ARL in 2009 because of winter kill, cumulative 2010–2011 emissions were similar at both sites. Across both sites, N_2O emissions relative to aboveground yield of continuous corn were slightly greater than the rotation (0.88), switchgrass (0.67), and early successional community (0.79). The emissions relative to yield in native grasses were just under half that of continuous corn (0.43), while the restored prairie (0.18), miscanthus (0.15), and poplar (0.14) were the lowest.

Annual nitrous oxide emissions by year and site

We analyzed annual N_2O emissions separately by *year* and *site* (Fig. 2) due to a significant *site* × *year* × *cropping system* interaction ($P < 0.001$). For 2009 treatment comparisons, model selection indicated that continuous corn and miscanthus at KBS were not significantly different and had the highest emissions, followed by the rotational phase of corn and poplar; all other systems had emissions that were not significantly different from each other (Fig. 2a). The treatments responded differently at ARL where the corn phase of the rotation had more than twice the emissions of continuous corn. After continuous corn and the corn phase of the rotation, there were no differences among other systems with the exception of restored prairie, which had the lowest emissions (Fig. 2b).

The general patterns of emissions from treatments in 2010 were similar at both sites. Continuous corn and the corn phase of the rotation had the highest emissions at both KBS and ARL (Fig. 2c,d). Most systems at KBS had relatively low emissions (Fig. 2c), similar to emissions from native grass mix and restored prairie at ARL (Fig. 2d). With the exception of continuous corn, which was 21% higher at KBS, average emissions at ARL were 12% higher from annual systems, and 68% higher from perennial systems than the respective treatments at KBS.

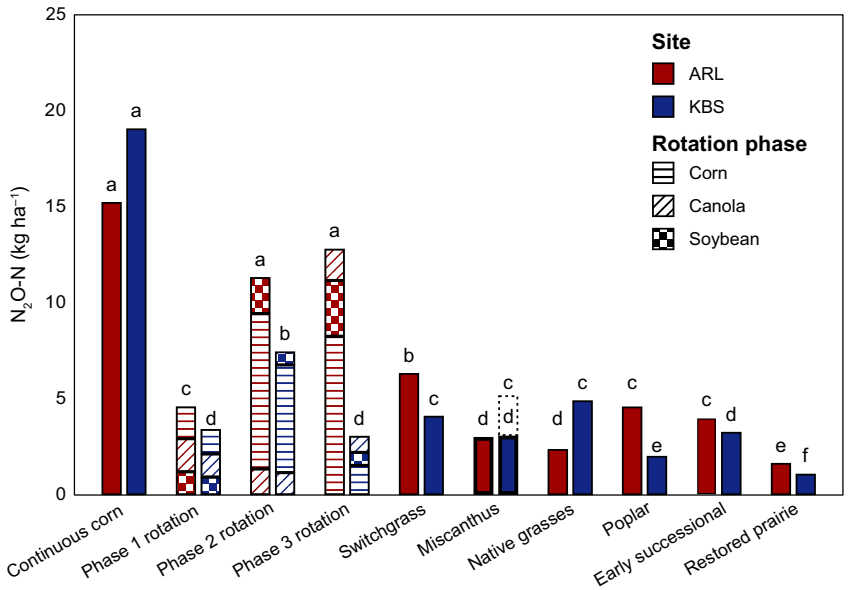

Fig. 1 Cumulative 2009–2011 N_2O fluxes from 8 bioenergy cropping systems grown at Arlington Agricultural Research Station, WI (ARL) and Kellogg Biological Station, MI (KBS). Values presented are geometric means with $n = 5$ at ARL and $n = 4$ at KBS. Phases of a corn–soybean–canola rotation are separated by the contribution of each specific rotation phase in ascending chronological order; analysis was conducted on the summed fluxes. Bars sharing a letter can be grouped during stepwise factor level collapse without significantly reducing the explanatory power of the model ($P > 0.05$). Miscanthus bars and letters correspond to 2010–2011 fluxes; for KBS, the dotted line and corresponding letter show the contribution of 2009 flux.

Emissions in 2011 differed from the patterns observed in previous years. At KBS, the highest emissions were from the native grasses, followed by continuous corn, which grouped with the switchgrass, miscanthus, and early successional community systems. Poplar, restored prairie, and the soybean phase of the rotation responded with the lowest emissions (Fig. 2e). At ARL, the switchgrass monoculture deviated from prior patterns and together with continuous corn averaged 34% higher emissions than the average across all phases of the rotation, 54% higher than miscanthus, poplar, and early successional community, and 82% higher than the average of the native grass mix and restored prairie systems (Fig. 2f).

Environmental predictors of daily nitrous oxide flux

ARL and KBS differed substantially in their soil moisture; water-filled pore space (WFPS) values at ARL were almost universally higher than at KBS (Table 1). Nevertheless, seasonal patterns within sites were largely similar, with reduced summer WFPS in 2009 and 2011, but sustained WFPS during the wet summer in 2010 (Fig. S1). Median NO_3^- and NH_4^+, as measured by resin strips, were similar at both sites although the range of values for both species observed at ARL was greater. Extractable values of NH_4^+ were very similar at KBS and ARL for both 2010 and 2011, but the range of values for extractable NO_3^- was again greater at ARL (Table 1).

The timings of precipitation events, fertilizer applications, and N_2O flux measurements varied among sites and years, with sharp increases in daily N_2O fluxes tending to occur when these events synchronized (Fig. 3). In 2011 at KBS, for instance, fertilization of most perennial crops was followed in rapid succession by a 10-mm precipitation event and a very large N_2O flux (Fig. 3f); aggregate annual emissions from perennial systems were very high at KBS that year (Fig. 2e). During the late spring and early summer, systems receiving no N fertilization tended to show limited changes in their emissions. By contrast, fluxes from corn systems varied over several orders of magnitude. N fertilization in corn (blue arrows, Fig. 3) preceded a sharp increase in N_2O emission; the sole exception occurred in 2011 at ARL, when there were no precipitation events between fertilization and the next flux measurement (Fig. 3e). The canola rotational phase and most perennial systems

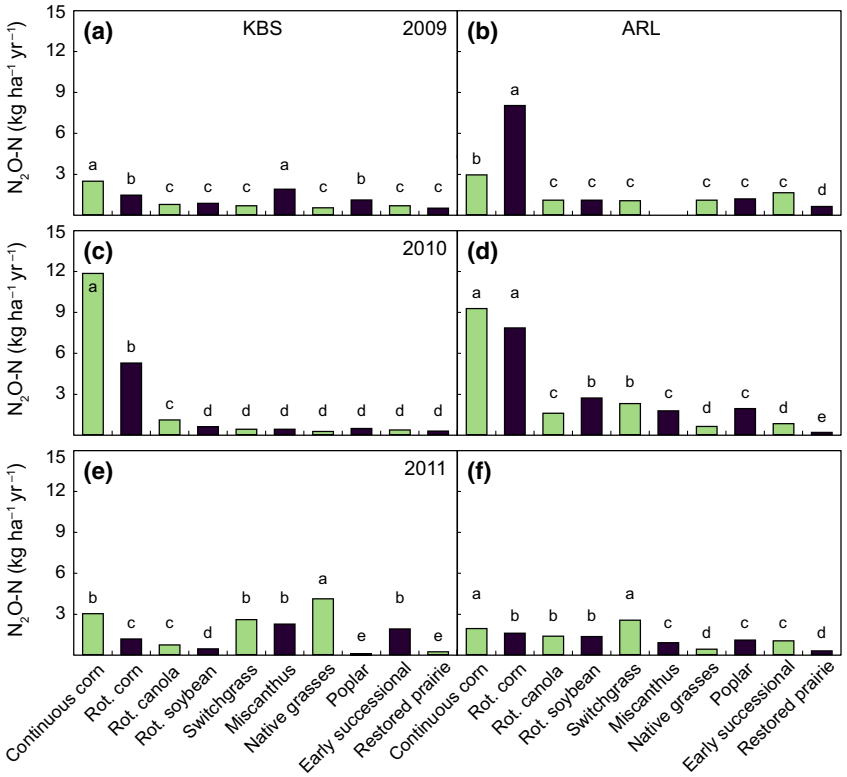

Fig. 2 Geometric mean of annual nitrous oxide emissions from the Biofuels Cropping System Experiment for the periods of 2009, 2010, and 2011. Left panels (a, c, and e) show results from KBS, $n = 4$, and right panels (b, d and f) show results from ARL, $n = 5$. See Fig. 1 legend for further information.

Table 1 Environmental factors observed at the GLBRC Bioenergy Cropping System Experiment colocated in Michigan (KBS) and Wisconsin (ARL)

				NH_4^+		NO_3^-	
Year	Site	Soil temp (°C)	WFPS (%)	Resin strip (μg N cm^{-2} day^{-1})	Soil pool (μg N g^{-1} soil)	Resin strip (μg N cm^{-2} day^{-1})	Soil pool (μg N g^{-1} soil)
2009	KBS	12.5 (3.0–22.0)	20 (7–29)	0.010 (0.002–0.071)		0.38 (0.03–3.68)	
	ARL	13.7 (1.1–23.3)	71 (40–89)	0.008 (0.001–0.149)		0.39 (0.04–5.59)	
2010	KBS	14.0 (5.4–21.0)	20 (13–27)		2.9 (0.7–12.6)		2.6 (1.5–5.3)
	ARL	15.5 (2.9–22.8)	72 (53–93)		3.7 (1.9–17.4)		5.3 (0.9–56.3)
2011	KBS	15.0 (4.0–23.5)	22 (9–31)		1.7 (0.7–7.7)		2.3 (1.3–4.4)
	ARL	15.0 (−0.4–25.0)	67 (37–83)		1.7 (0.9–7.7)		2.7 (0.4–25.2)

Median values are presented, with 5th and 95th percentile values in parentheses. Sites were Arlington Agricultural Research Station, WI (ARL) and Kellogg Biological Research Station, MI (KBS). WFPS is water-filled pore space.

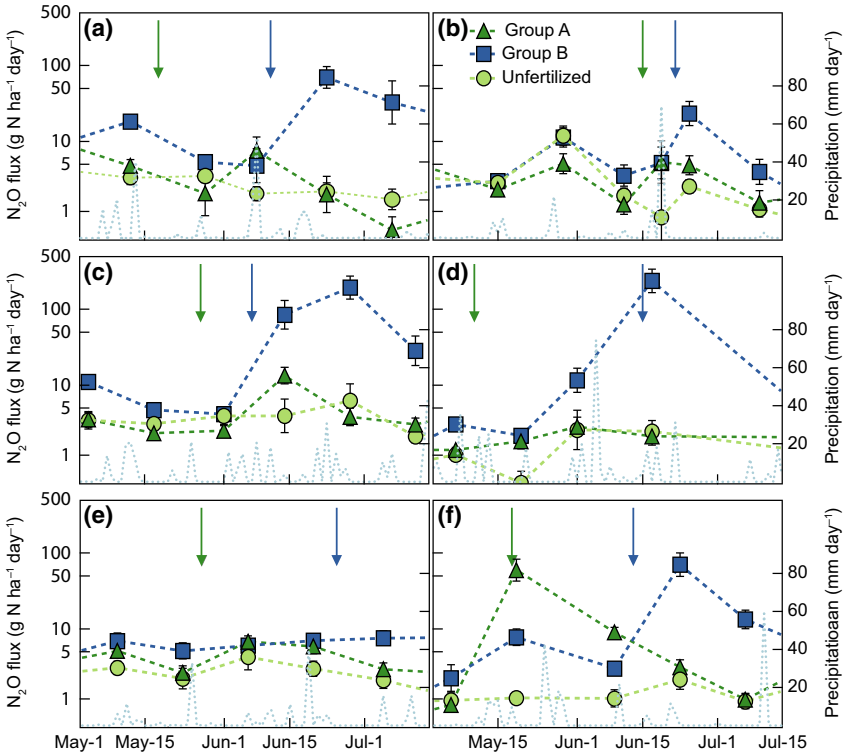

Fig. 3 Average daily precipitation and nitrous oxide flux during late spring/early summer. Data presented separately by site and year: (a) 2009 ARL, (b) 2009 KBS, (c) 2010 ARL, (d) 2010 KBS, (e) 2011 ARL, and (f) 2011 KBS. All treatments within a group were fertilized at the same time, denoted by arrows. Group A (gray arrow) consisted of rotational canola, early successional community, switchgrass (post-2009), native grasses (post-2009), poplar (2010 only), and miscanthus (2010 at KBS, 2011 both sites). Group B (black arrow) consisted of continuous and rotational corn and miscanthus (2009 at KBS). Unfertilized treatments included rotational soybeans, restored prairie, poplar (except 2010), switchgrass (2009 only), native grasses (2009 only), and miscanthus (2010 at ARL). Data are presented with inverse hyperbolic sine scaling, with error bars ± 1 SE.

were fertilized earlier in the year and at a lower rate than corn (Table S1; gray arrows, Fig. 3). The range of emissions from these systems tended to be lower than for corn, as were the emission increases following fertilization events. Our data are too limited to broadly infer a generalized relationship between precipitation amounts and subsequent N_2O fluxes, but we note that in all cases where N_2O flux increased sharply after fertilization there was at least one precipitation event of 10 mm or more between

fertilization and flux measurement, whereas among the cases where fertilization was not followed by a large flux increase, there was only one instance where a precipitation event of more than 10 mm was observed prior to flux measurement (Fig. 3a, Group A).

Bayesian model averaging of environmental predictors

Models trained on specific systems varied greatly in their capacity to explain variation in both their training data and the full data (Table 2). Specifically, poplar, miscanthus, and systems containing corn were relatively well modeled while the polycultures (native grasses, early successional community, and restored prairie) were not. There were no environmental factors that substantially contributed to model fits across all systems (Table S2). There were also substantial differences in how well models trained on a given system predicted fluxes from other systems (Table S3). This relationship was not reciprocal. For example, the model based on data from native grass system predicted fluxes from poplar system better than the model based on poplar data predicted fluxes from native grasses.

We tested how effectively models trained on specific systems captured the temporal dynamics of fluxes from their own and other systems (Fig. 4). Flux dynamics at ARL were better modeled than those from KBS, where the models failed to predict major emission events (Fig. 4d–f). Despite the high correlation between predictions from the corn and native grass-based models ($R^2 = 0.58$), actual values from the native grass model were systematically lower than those from the corn model. The switchgrass-based model was inconsistent in its relationship to the other two models, sometimes tracking the corn model (Fig. 4b,d) and at other times the native grass model (Fig. 4f). Overall, each model's performance was poor on systems other than the one on which it had been trained.

Table 2 Bayesian model averaged posterior probabilities of inclusion for environmental factors used to predict N_2O fluxes

	Training dataset							
Factor	Full data	Corn	Miscanthus	Native grasses	Early successional community	Poplar	Restored Prairie	Switchgrass
Site	1.00	1.00	0.53	0.60	0.25	1.00	0.03	0.17
Year	0.61	0.23	0.01	0.05	0.03	0.02	0.19	0.12
NH_4^+	0.81	0.06	0.13	0.01	0.04	0.09	0.05	0.90
NO_3^-	0.95	0.05	0.12	0.54	0.53	0.04	0.12	0.04
Soil temperature (ST)	0.00	0.27	0.23	0.24	0.04	0.04	0.01	0.14
$WFPS_C$	0.03	0.02	0.04	0.12	0.07	0.02	0.03	0.07
Site × Year	0.00	0.02	0.05	0.82	0.03	0.01	0.04	0.02
Site × NH_4^+	1.00	0.29	0.05	0.01	0.02	0.04	0.18	1.00
Site × NO_3^-	1.00	0.02	0.04	0.32	0.78	0.01	0.06	0.96
Site × ST	1.00	1.00	0.55	0.61	1.00	0.01	0.03	0.20
Site × $WFPS_C$	0.00	0.57	0.02	0.01	0.38	0.21	0.07	0.05
Year × NH_4^+	0.68	0.01	0.01	0.08	0.03	0.05	0.02	0.02
Year × NO_3^-	1.00	0.03	0.02	0.01	0.75	0.10	0.04	0.89
Year × ST	0.00	0.19	0.02	0.17	0.03	0.02	0.02	0.07
Year × $WFPS_C$	1.00	0.01	0.50	0.05	0.09	0.69	0.02	0.02
NH_4^+ × NO_3^-	0.00	0.09	0.08	0.02	0.16	0.02	0.04	0.02
NH_4^+ × ST	1.00	0.03	0.07	0.01	0.12	0.23	0.03	0.90
NH_4^+ × $WFPS_C$	0.06	1.00	0.01	0.01	0.02	0.03	0.02	0.02
NO_3^- × ST	0.08	0.76	0.86	0.42	0.43	0.87	0.03	0.02
NO_3^- × $WFPS_C$	1.00	0.01	0.75	0.06	0.04	0.01	0.04	0.02
ST × $WFPS_C$	1.00	0.03	0.99	0.95	0.09	1.00	0.03	0.96
Training R^2	0.33	0.46	0.39	0.21	0.17	0.52	0.06	0.27
Full data R^2	0.33	0.22	0.27	0.24	0.07	0.22	0.02	0.20

Models were trained on N_2O flux data obtained from individual cropping systems. NH_4^+ and NO_3^- concentrations were log-transformed for analysis. The two sites were Arlington Agricultural Research Station (ARL) and Kellogg Biological Research Station (KBS). $WFPS_C$ is water-filled pore space scaled and centered separately for each site. See Table S2 for factor coefficients and probabilities for all cropping systems.

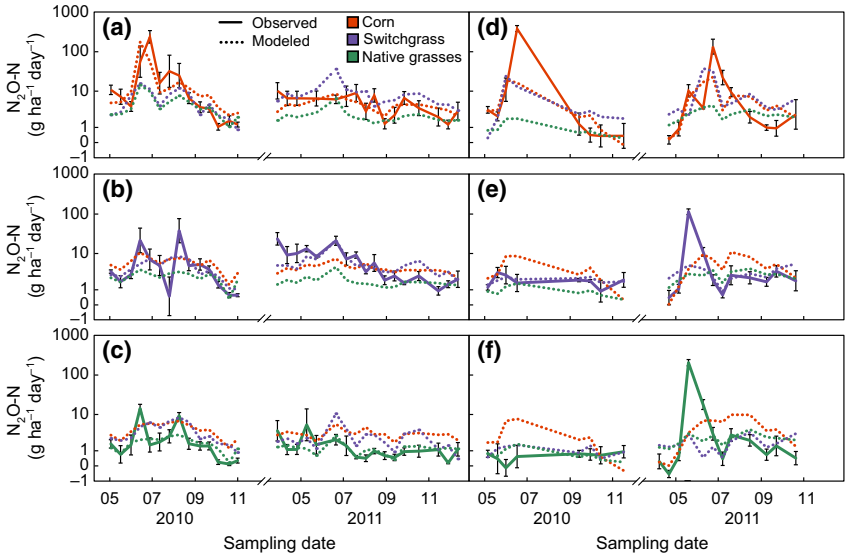

Fig. 4 Observed and modeled daily N_2O fluxes at ARL and KBS. Solid lines indicate mean observed N_2O fluxes of: (a) continuous corn ARL, (b) switchgrass ARL, (c) native grasses ARL, (d) continuous corn KBS, (e) switchgrass KBS, and (f) native grasses KBS. Dotted lines indicate mean daily predictions from models trained on data collected from the three cropping systems. The vertical axis has inverse hyperbolic sine scaling, which asymptotically approaches logarithmic scaling. Error bars indicate ±1 SE. A 90-day period during which no fluxes were measured was removed from the horizontal axis to conserve space.

Discussion

Cropping systems that included corn were consistently higher in N_2O emissions for any given site year, notwithstanding a high degree of interannual variability. With few exceptions, N_2O emissions from fertilized perennial systems were much lower than annual systems, while those from unfertilized restored prairie were lowest overall.

Previous work has demonstrated that rate of N fertilizer application has a strong influence on N_2O emissions from both annual and perennial systems (Dobbie *et al.*, 1999; Millar *et al.*, 2010). The percentage of applied fertilizer emitted as N_2O varies with site conditions and management, but, in general, N_2O emissions are highest where inorganic N is readily available. This is reflected in emissions from the continuous corn system which received ~ 3*x* the rate of N (160 kg ha^{-1}) as the fertilized perennial systems (56 kg ha^{-1}). Other factors such as crop rotation (i.e., crop diversity) can influence N_2O emission rates. Crop rotation is often associated with reduced N demand which results in reduced N inputs and N_2O emissions (Drury *et al.*, 2008; Osterholz *et al.*, 2014). The effect of crop rotation in our study was less clear with cumulative emissions being highly dependent on climatic conditions during the corn phase, indicating a strong interaction between crop phase and year.

Cumulative N_2O emissions can be driven by short-duration, high-intensity flux events (Molodovskaya *et al.*, 2012). These events typically occur when coincidence of fertilization and precipitation results in limited soil oxygen and readily available reactive N (Dobbie & Smith, 2003; Castellano *et al.*, 2010; Matthews *et al.*, 2010). In general, we observed this pattern, where nearly concurrent fertilization and precipitation events resulted in substantial emissions spikes; of all the fertilized systems, this effect was most clearly observed in corn while emissions for crops grown in the absence of fertilizer were almost invariant throughout this period at ARL and were only slightly variable at KBS.

The difference in cumulative N_2O emissions between ARL and KBS is likely driven by soil properties. Soils at the two sites differed in both their order and texture, with ARL soils consisting of fine textured mollisols and KBS a coarser-textured alfisol. Of the two soil orders, mollisols are typically associated with higher carbon and nutrient contents, consistent with the higher carbon and inorganic N values recorded at ARL. Given that both sites received comparable precipitation, greater WFPS at ARL appears to stem from greater water-holding capacity emerging from high soil organic matter and finer soil texture. We thus attribute the consistently higher emissions at ARL to soil moisture-driven increases in anaerobic microsite abundance and longevity (Bouwman, 1996) coupled with greater N and C availability. Our findings are consistent with studies in both agricultural and wildland ecosystems that have linked finer soil texture and greater soil carbon

availability to increased N_2O emissions (Bouwman *et al.*, 2002; Stehfest & Bouwman, 2006). While the restored prairie system was not fertilized at either site, greater soil C at ARL suggests potential for rapidly mineralizing N, and this coupled with higher WFPS, may have facilitated the slightly higher fluxes observed at ARL. In contrast, between-site differences in the poplar system were at least partially attributable to an infestation of the ARL plots with the fungal leaf pathogen marssonina (*Marssonina populi* (Lib.) Magnus). The infestation peaked in mid-August 2010 leading to complete defoliation by 15 September; this likely reduced plant N uptake in the only year that N fertilizer was applied to poplar, leaving more N available for microbial conversion and loss as N_2O.

Cropping systems based on perennial species require multiple years to become fully established (Parrish & Fike, 2005). This development is most evident in the delay in attaining maximum yields, but N-cycling processes may also change during this period (Smith *et al.*, 2013; Lesur *et al.*, 2014). During the period of this study, N_2O emissions per unit aboveground yield were much lower in the perennial systems. It is likely this ratio will improve as the systems come into full production phase and as farmers become more efficient, both in harvest timing and mechanical efficiency, at harvesting perennial biomass. Perennial systems also produce greater biomass belowground which over time will likely improve soil organic matter and site fertility. While our study was not structured to explicitly explore the effects of the establishment period, it is still a potentially relevant contextual element for interpreting results from the perennial cropping systems. Our results were largely comparable to studies of perennial systems similarly conducted over the establishment phase (Hernandez-Ramirez *et al.*, 2009; Smith *et al.*, 2013). However, given the high influence of interannual variability on our results, it is clear that long-term studies will be required to bound this variability and determine whether establishment-phase N_2O emissions are representative of established perennial cropping systems.

A consideration for our results is that our study lacked measurements during winter (December–February), which could have resulted in underestimation of N_2O emissions. Substantial N loss can occur during this fallow period, especially in conventionally managed annual row crops when bare soil is subjected to freeze–thaw events (Johnson *et al.*, 2010). Soil N is susceptible to denitrification during this period, especially for systems where manure has been applied after the primary crop has been harvested (Parkin *et al.*, 2006), or where vegetative cover is not present during winter (McSwiney *et al.*, 2010). However, only our annual cropping systems had significant bare soil during winter, and as discussed above, N_2O emissions in these systems were dominated by relatively brief spikes following fertilizer events. Nitrogen was not applied in the fall to any of our cropping systems so we expect that winter measurements would have negligible influence on the magnitude and comparison of N_2O emissions.

The Bayesian averaged models we analyzed in detail suggested alternative cropping systems would produce different N_2O fluxes under a given set of environmental conditions. Our statistical models based on emissions measured from our various cropping systems had very distinct parameterizations, even when the systems were as similar as continuous and rotational corn. Previous studies have similarly found that key environmental predictors of N_2O emissions vary among systems (Dechow & Freibauer, 2011; Imer *et al.*, 2013). The BMA based on switchgrass, for instance, frequently predicted substantially higher emissions than the model based on native grasses, implying that at a given soil moisture, soil temperature, and inorganic N concentration, switchgrass and native grasses would have different N_2O emissions. Cropping systems may differ not only in their effect on environmental parameters (e.g., through crop species differences in N uptake and water use), but also in their response to these parameters. The role of plant community composition and diversity in determining trace gas fluxes from soil has received little attention (but see Hoeft *et al.*, 2012).

Given our results, there may be a significant gap in our ability to account for how plant community composition influences the response of N_2O fluxes to environmental drivers. Single-species monocultures have typically been used to model the broader category of herbaceous biomass crops (Surendran Nair *et al.*, 2012), with switchgrass used as a model for exploring the properties and environmental responses of bioenergy crops (Lewandowski *et al.*, 2003; Tulbure *et al.*, 2012). The cropping system specificity we observed in the response of N_2O fluxes to environmental parameters suggests it may be risky to rely on model systems to predict the behaviors of perennial and polycultural biomass cropping systems, particularly with the potential for high variability during the establishment phase.

In summary, across years with highly variable climate, N_2O emissions were consistently higher from annual than perennial cropping systems. Under particular conditions, namely rainfall following fertilizer, emissions from corn dwarfed all other systems. N_2O emissions were consistently low for unfertilized restored prairie harvested for biomass. Perennial cropping systems on highly productive mollisols had higher N_2O emissions than the same systems growing on moderately productive alfisols. Finally, N_2O flux responses to environmental conditions during establishment were

not generalizable across cropping systems, indicating that use of model systems, especially for perennials and polycultures, should be performed cautiously.

Acknowledgements

We thank S. Hamilton, A. Dean, J. Tesmer, J. Sustachek, N. Tautges, A. Miller, Z. Andersen, B. Faust, K. Kahmark, S. VanderWulp, and many others for assistance in the field and laboratory. We also thank S. Bohm for providing the FluxQC framework, S. Sippel for database management, and anonymous reviewers for comments that improved the manuscript. Funding was provided by the DOE Great Lakes Bioenergy Research Center (DOE BER Office of Science DE-FC02-07ER64494) and the DOE OBP Office of Energy Efficiency and Renewable Energy (DE-AC05-76RL01830), and at KBS the NSF Long-term Ecological Research Program and Michigan State University AgBioResearch.

References

Adler PR, Del Grosso SJ, Parton WJ (2007) Life-cycle assessment of net greenhouse-gas flux for bioenergy cropping systems. *Ecological Applications*, **17**, 675–691.

Anderson-Teixeira KJ, Masters MD, Black CK, Zeri M, Hussain MZ, Bernacchi CJ, DeLucia EH (2013) Altered belowground carbon cycling following land-use change to perennial bioenergy crops. *Ecosystems*, **16**, 508–520.

Bouwman AF (1996) Direct emission of nitrous oxide from agricultural soils. *Nutrient Cycling in Agroecosystems*, **46**, 53–70.

Bouwman AF, Boumans LJM, Batjes NH (2002) Emissions of N_2O and NO from fertilized fields: summary of available measurement data. *Global Biogeochemical Cycles*, **16**, 6-1–6-13.

Bouwman AF, Van Grinsven JJM, Eickhout B (2010) Consequences of the cultivation of energy crops for the global nitrogen cycle. *Ecological Applications*, **20**, 101–109.

Burbidge JB, Magee L, Robb AL (2013) Alternative transformations to handle extreme values of the dependent variable. *Journal of the American Statistical Association*, **83**, 123–127.

Castellano MJ, Schmidt JP, Kaye JP, Walker C, Graham CB, Lin H, Dell CJ (2010) Hydrological and biogeochemical controls on the timing and magnitude of nitrous oxide flux across an agricultural landscape. *Global Change Biology*, **16**, 2711–2720.

Cavigelli MA, Robertson GP (2001) Role of denitrifier diversity in rates of nitrous oxide consumption in a terrestrial ecosystem. *Soil Biology and Biochemistry*, **33**, 297–310.

Chen D, Li Y, Grace P, Mosier AR (2008) N_2O emissions from agricultural lands: a synthesis of simulation approaches. *Plant and Soil*, **309**, 169–189.

Crum JR, Collins HP (1995) *KBS Soils*. Kellogg Biological Station Long-Term Ecological Research, Michigan State University, Hickory Corners, MI. Available at: http://lter.kbs.msu.edu/research/site-description-and-maps/soil-description (accessed 19 September 2014).

Dale VH, Kline KL, Wright LL, Perlack RD, Downing M, Graham RL (2011) Interactions among bioenergy feedstock choices, landscape dynamics, and land use. *Ecological Applications*, **21**, 1039–1054.

Dale BE, Anderson JE, Brown RC *et al.* (2014) Take a closer look: biofuels can support environmental, economic and social goals. *Environmental science and Technology*, **48**, 7200–7203.

Dechow R, Freibauer A (2011) Assessment of German nitrous oxide emissions using empirical modelling approaches. *Nutrient Cycling in Agroecosystems*, **91**, 235–254.

Dobbie K, Smith K (2003) Nitrous oxide emission factors for agricultural soils in Great Britain: the impact of soil water-filled pore space and other controlling variables. *Global Change Biology*, **9**, 204–218.

Dobbie KE, McTaggart IP, Smith KA (1999) Nitrous oxide emissions from intensive agricultural systems: variations between crops and seasons, key driving variables, and mean emission factors. *Journal of Geophysical Research*, **104**, 26891.

Drury CF, Yang XM, Reynolds WD, McLaughlin NB (2008) Nitrous oxide and carbon dioxide emissions from monoculture and rotational cropping of corn, soybean and winter wheat. *Canadian Journal of Soil Science*, **88**, 163–174.

Gelfand I, Zenone T, Jasrotia P, Chen J, Hamilton SK (2011) Carbon debt of Conservation Reserve Program (CRP) grasslands converted to bioenergy production. *Proceedings of the National Academy of Sciences*, **108**, 13864–13869.

Henault C, Bizouard F, Laville P, Gabrielle B, Nicoullaud B, Germon JC, Cellier P (2005) Predicting *in situ* soil N_2O emission using NOE algorithm and soil database. *Global Change Biology*, **11**, 115–127.

Hernandez-Ramirez G, Brouder SM, Smith DR, Van Scoyoc GE (2009) Greenhouse gas fluxes in an eastern Corn Belt soil: weather, nitrogen source, and rotation. *Journal of Environmental Quality*, **38**, 841–854.

Hoeft I, Steude K, Wrage N, Veldkamp E (2012) Response of nitrogen oxide emissions to grazer species and plant species composition in temperate agricultural grassland. *Agriculture, Ecosystems and Environment*, **151**, 34–43.

Hoeting JA, Madigan D, Raftery AE, Volinsky CT (1999) Bayesian model averaging: a tutorial. *Statistical Science*, **14**, 382–417.

Hutchinson GL, Mosier AR (1981) Improved soil cover method for field measurement of nitrous oxide fluxes. *Soil Science Society of America Journal*, **45**, 311.

Imer D, Merbold L, Eugster W, Buchmann N (2013) Temporal and spatial variations of soil CO_2, CH_4 and N_2O fluxes at three differently managed grasslands. *Biogeosciences*, **10**, 5931–5945.

Johnson JMF, Archer D, Barbour N (2010) Greenhouse gas emission from contrasting management scenarios in the northern Corn Belt. *Soil Science Society of America Journal*, **74**, 396–406.

Jokela W, Posner J, Hedtcke J, Balser T, Read H (2011) Midwest cropping system effects on soil properties and on a soil quality index. *Agronomy Journal*, **103**, 1552–1562.

Lesur C, Bazot M, Bio-Beri F, Mary B, Jeuffroy M-H, Loyce C (2014) Assessing nitrate leaching during the three-first years of *Miscanthus* × *giganteus* from on-farm measurements and modeling. *GCB Bioenergy*, **6**, 439–449.

Lewandowski I, Scurlock JMO, Lindvall E, Christou M (2003) The development and current status of perennial rhizomatous grasses as energy crops in the US and Europe. *Biomass and Bioenergy*, **25**, 335–361.

Maroja LS, Andrés JA, Walters JR, Harrison RG (2009) Multiple barriers to gene exchange in a field cricket hybrid zone. *Biological Journal of the Linnean Society*, **97**, 390–402.

Matthews RA, Chadwick DR, Retter AL, Blackwell MSA, Yamulki S (2010) Nitrous oxide emissions from small-scale farmland features of UK livestock farming systems. *Agriculture, Ecosystems and Environment*, **136**, 192–198.

McLaughlin SB, Adams Kszos L (2005) Development of switchgrass (*Panicum virgatum*) as a bioenergy feedstock in the United States. *Biomass and Bioenergy*, **28**, 515–535.

McSwiney CP, Snapp SS, Gentry LE (2010) Use of N immobilization to tighten the N cycle in conventional agroecosystems. *Ecological Applications*, **20**, 648–662.

Millar N, Robertson GP, Grace PR, Gehl RJ, Hoben JP (2010) Nitrogen fertilizer management for nitrous oxide (N_2O) mitigation in intensive corn (Maize) production: an emissions reduction protocol for US Midwest agriculture. *Mitigation and Adaptation Strategies for Global Change*, **15**, 185–204.

Molodovskaya M, Singurindy O, Richards BK, Warland J, Johnson MS, Steenhuis TS (2012) Temporal variability of nitrous oxide from fertilized croplands: hot moment analysis. *Soil Science Society of America Journal*, **76**, 1728.

MSCO (2013) Michigan State Climatologist's Office: 27 year summary of annual values for Gull Lake (3504) 1981–2010, Available at: http://climate.geo.msu.edu/climate_mi/stations/3504/1981-2010%20annual%20summary.pdf (accessed 2 April 2014).

Nikièma P, Rothstein DE, Min D-H, Kapp CJ (2011) Nitrogen fertilization of switchgrass increases biomass yield and improves net greenhouse gas balance in northern Michigan, USA. *Biomass and Bioenergy*, **35**, 4356–4367.

Nikièma P, Rothstein DE, Miller RO (2012) Initial greenhouse gas emissions and nitrogen leaching losses associated with converting pastureland to short-rotation woody bioenergy crops in northern Michigan, USA. *Biomass and Bioenergy*, **39**, 413–426.

NWS (2013) National Weather Service: Wisconsin 30 year avereage temperature and precipitation 1981–2010, Available at: www.crh.noaa.gov/images/mkx/climate/avg_30_year_precip.png and www.crh.noaa.gov/images/mkx/climate/avg_30_year_temp.png (accessed 2 April 2014).

Osterholz WR, Kucharik CJ, Hedtcke JL, Posner JL (2014) Seasonal nitrous oxide and methane fluxes from grain- and forage-based production systems in Wisconsin, USA. *Journal of Environment Quality*, **43**, 1833–1843.

Palmer MM, Forrester JA, Rothstein DE, Mladenoff DJ (2014) Conversion of open lands to short-rotation woody biomass crops: site variability affects nitrogen cycling and N_2O fluxes in the US Northern Lake States. *GCB Bioenergy*, **6**, 450–464.

Parkin TB, Kaspar TC, Singer JW (2006) Cover crop effects on the fate of N following soil application of swine manure. *Plant and Soil*, **289**, 141–152.

Parrish DJ, Fike JH (2005) The biology and agronomy of switchgrass for biofuels. *Critical Reviews in Plant Sciences*, **24**, 423–459.

Pedersen AR (2011) 'HMR': Flux estimation with static chamber data. R package version 0.3.1.

Pinheiro J, Bates D, DebRoy S, Sarkar D, The R Core Team (2013) nlme: Linear and Nonlinear Mixed Effects Models. R package version 3.1.

R Core Team (2014) R: A language and environment for statistical computing. R Foundation for Statistical Computing, Vienna, Austria. URL http://www.R-project.org/.

Raftery AE, Hoeting JA, Volinsky CT, Painter I, Yeung KY, (2013) *BMA: Bayesian Model Averaging*. R package version 3.16.2.2. Available: http://cran.r-project.org/package=BMA (accessed 25 September 2013).

Reay DS, Davidson EA, Smith KA, Smith P, Melillo JM, Dentener F, Crutzen PJ (2012) Global agriculture and nitrous oxide emissions. *Nature Climate Change*, **2**, 410–416.

Robertson GP, Groffman PM (2015) Nitrogen transformations. In: *Soil Soil Microbiology, Ecology and Biochemistry* (ed. Paul EA), pp. 421–446. Academic Press, Burlington, MA.

Robertson GP, Coleman DC, Bledsoe CS, Sollins P (eds.) (1999) *Standard Soil Methods for Long-Term Ecological Research*, pp. 1–462. Oxford University Press, New York.

Robertson GP, Paul EA, Harwood RR, (2000) Greenhouse gases in intensive agriculture: contributions of individual gases to the radiative forcing of the atmosphere. *Science*, **289**, 1922–1925.

Robertson GP, Dale VH, Doering OC *et al*. (2008) Sustainable biofuels redux. *Science*, **322**, 49–50.

Robertson GP, Bruulsema TW, Gehl RJ, Kanter D, Mauzerall DL, Rotz CA, Williams CO (2012) Nitrogen–climate interactions in US agriculture. *Biogeochemistry*, **114**, 41–70.

Ruan L, Robertson GP (2013) Initial nitrous oxide, carbon dioxide, and methane costs of converting conservation reserve program grassland to row crops under no-till vs. conventional tillage. *Global Change Biology*, **19**, 2478–2489.

Sanderson MA, Adler PR (2008) Perennial forages as second generation bioenergy crops. *International Journal of Molecular Sciences*, **9**, 768–788.

Sanford GR, Posner JL, Jackson RD, Kucharik CJ, Hedtcke JL, Lin T-L (2012) Soil carbon lost from Mollisols of the North Central USA with 20 years of agricultural best management practices. *Agriculture, Ecosystems and Environment*, **162**, 68–76.

Schlesinger WH (2013) An estimate of the global sink for nitrous oxide in soils. *Global Change Biology*, **19**, 2929–2931.

Smith KA, Dobbie KE (2001) The impact of sampling frequency and sampling times on chamber-based measurements of N_2O emissions from fertilized soils. *Global Change Biology*, **7**, 933–945.

Smith CM, David MB, Mitchell CA, Masters MD, Anderson-Teixeira KJ, Bernacchi CJ, DeLucia EH (2013) Reduced nitrogen losses after conversion of row crop agriculture to perennial biofuel crops. *Journal of Environment Quality*, **42**, 219.

Stehfest E, Bouwman L (2006) N_2O and NO emission from agricultural fields and soils under natural vegetation: summarizing available measurement data and modeling of global annual emissions. *Nutrient Cycling in Agroecosystems*, **74**, 207–228.

Surendran Nair S, Kang S, Zhang X *et al*. (2012) Bioenergy crop models: descriptions, data requirements, and future challenges. *GCB Bioenergy*, **4**, 620–633.

Tulbure MG, Wimberly MC, Boe A, Owens VN (2012) Climatic and genetic controls of yields of switchgrass, a model bioenergy species. *Agriculture, Ecosystems and Environment*, **146**, 121–129.

Zenone T, Chen J, Deal MW *et al*. (2011) CO_2 fluxes of transitional bioenergy crops: effect of land conversion during the first year of cultivation. *GCB Bioenergy*, **3**, 401–412.

Supporting Information

Additional Supporting Information may be found in the online version of this article:

Figure S1. Average soil temperature and water-filled pore space at ARL and KBS over the study period.

Tables S1–S3. Tables providing agronomic management details, BMA analysis results for all cropping systems, and correlations between predicted and observed N_2O fluxes using different cropping systems as training data.

Appendix S1. Detailed description of statistical analyses.

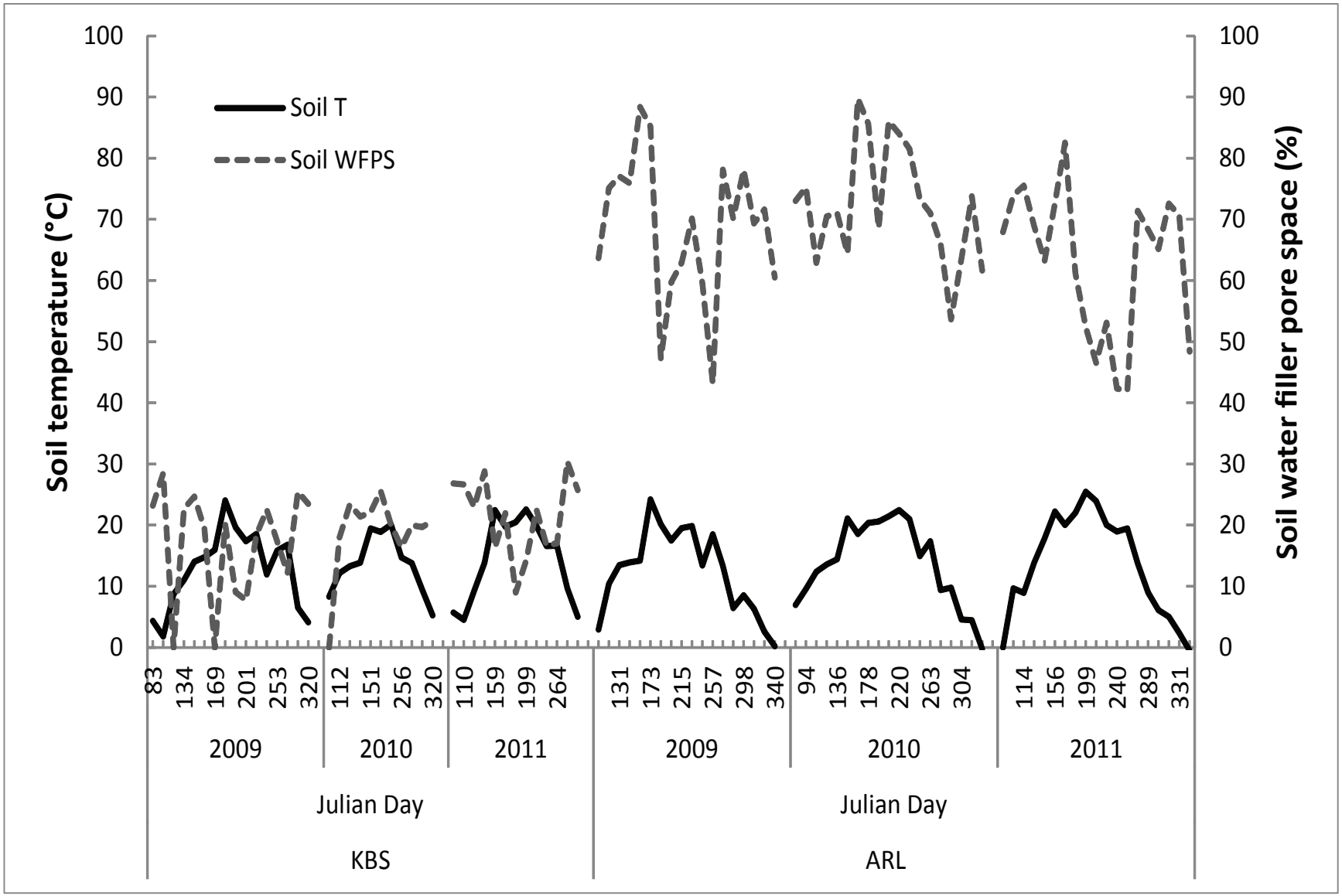
Soil T
Soil WFPS
Soil temperature (°C)
Soil water filler pore space (%)
100
90
80
70
60
50
40
30
20
10
0
83
134
169
201
253
320
112
151
256
320
110
159
199
264
131
173
215
257
298
340
94
136
178
220
263
304
114
156
199
240
289
331
2009
2010
2011
2009
2010
2011
Julian Day
Julian Day
KBS
ARL

Table S1. Crop characteristics and agronomic management of the Bioenergy Cropping System Experiment (BCSE) at Arlington, WI (ARL), and Hickory Corners, MI (KBS). Four year average planting date, seeding rate, and N application rate are included for continuous corn and the corn, soybean and canola phases of the rotation.

System		crop	site	planting date	crop and variety[1]	seeding rate[2]	N rate (kg ha^{-1})	first N application
1		cont. corn	ARL KBS	May 5	corn *(Zea mays* L.): DK5259, P35F40, DK5259, DK5259, P35F40 corn: DK5259, DK5259, DK5259, DK5259, DK5259	84,000 sds ha^{-1} 70,900 sds ha^{-1}	150 168	2008 2008
2,3,4	Rotation	corn soybean canola	AARS KBS	May 5 May 5 April 15	corn *(Zea mays* L.): DK5259 soybean (*Glycine max* [L.] Merr.): Pioneer 92M40; Pioneer 92Y30 canola (*Brassica napus* L.): DKL 5210	84,000; 70,900 sds ha^{-1} 170,000; 180,000 sds ha^{-1} 2.7; 4.4 kg ha^{-1}	150;160 0 70	2008 n/a 2008
5		switchgrass	ARL KBS	June 24, 2008 June 19, 2008[3]	switchgrass (*Panicum virgatum* L.), "Cave-In-Rock"	14 kg ha^{-1}	56	2010
6		miscanthus	ARL KBS	May 13, 2008[4] May 21, 2008	*Miscanthus x giganteus*, "Illinois clone"	17,200 rhizomes ha^{-1}	56	2011 2009
7		native grasses	ARL KBS	June 24, 2008 June 19, 2008	big bluestem (*Andropogon gerardii* Vitman) Canada wild rye (*Elymus Canadensis* L.) indiangrass (*Sorghastrum nutans* [L.] Nash) little bluestem (*Schizachyrium scoparium* [Michx.] Nash) switchgrass, "Southlow"	2.4 kg ha^{-1} 1.6 kg ha^{-1} 2.4 kg ha^{-1} 3.2 kg ha^{-1} 1.6 kg ha^{-1}	56	2010
8		poplar	ARL KBS	May 9, 2008 May 1, 2008	NM-6 hybrid poplar (*Populus nigra* x *Populus maximowiczii*)	2,630 trees ha^{-1}	213 157	2010
9		old field	ARL KBS	n/a	plant community defined by pre-existing seed bank and novel recruitment	n/a	56	2009
10		restored prairie	ARL KBS	June 24, 2008 June 19, 2008[6]	**grasses** big bluestem Canada wild rye indiangrass junegrass (*Koeleria cristata* [Ledeb.] Schult.) little bluestem switchgrass, "Southlow" **leguminous forbes** roundhead bushclover (*Lespedeza capitata* Michx.) showy tick-trefoil (*Desmodium canadense* (L.) DC.) white wild indigo (*Baptisia leucantha* Torr. & Gray) **non-leguminous forbes** black-eyed susan (*Rudbeckia hirta* L.) butterfly weed (*Asclepias tuberosa* L.) cup plant (*Silphium perfoliatum* L.) meadow anemone (*Aneomone canadensis* L.) New England aster (*Symphyotrichum novae-angliae* [L.] G.L. Nesom) pinnate prairie coneflower (*Ratibida pinnata* [Vent.] Barnhart) showy goldenrod (*Solidago speciosa* Nutt.) stiff goldenrod (*Solidago rigida* L.) wild bergamot (*Monarda fistulosa* L.)	 1.2 kg ha^{-1} 1.2 kg ha^{-1} 1.2 kg ha^{-1} 0.8 kg ha^{-1} 1.2 kg ha^{-1} 0.8 kg ha^{-1} 0.4 kg ha^{-1} 0.4 kg ha^{-1} 0.4 kg ha^{-1} 0.4 kg ha^{-1} 0.4 kg ha^{-1} 0.4 kg ha^{-1} 0.4 kg ha^{-1} 0.4 kg ha^{-1} 0.4 kg ha^{-1} 0.4 kg ha^{-1} 0.4 kg ha^{-1} 0.4 kg ha^{-1}	0	n/a

[1] Scientific and common names for each crop/species provided. For continuous corn and the corn, soybean, and canola phases of the rotation regionally appropriate hybrids were selected. Hybrid specifics are listed in order of season, 2008 to 2012.

[2] sds = seeds

[3] Spring flooding caused damage to 2008 planting. Stands were replanted on June 7, 2009

[4] 2008/2009 winter temperatures caused >95% stand loss, plots were re-planted on May 10, 2010. Nitrogen application did not begin until spring 2011.

Table S2. Bayesian model averaging inclusion probabilities and effect sizes for environmental predictors of aggregate annual soil N_2O emissions, by cropping system

	Full data			Continuous corn			Corn phase			Canola phase		
Factor	**Prob.**	**Est.**	**SE**	**Prob.**	**Est.**	**SE**	**Prob.**	**Est.**	**SE**	**Prob.**	**Est.**	**SE**
Intercept	1.00	1.2E+00	1.4E-01	1.00	1.5E+00	6.1E-01	1.00	1.9E+00	2.8E-01	1.00	1.1E+00	1.6E-01
Site	1.00	-1.1E+00	1.6E-01	1.00	-3.0E+00	5.1E-01	0.16	-9.0E-02	2.5E-01	0.02	2.6E-03	2.9E-02
Year	0.61	1.9E-01	1.7E-01	0.23	3.0E-01	6.5E-01	0.18	1.0E-01	2.7E-01	0.02	1.2E-03	2.3E-02
NO_3^-	0.95	1.9E-01	5.2E-02	0.05	4.1E-03	3.6E-02	0.01	-9.6E-05	6.9E-03	0.01	-7.7E-05	7.9E-03
NH_4^+	0.81	-2.8E-01	1.6E-01	0.06	-4.3E-02	2.3E-01	0.85	-5.0E-01	2.7E-01	0.70	3.1E-01	2.2E-01
ST	0.00	0.0E+00	0.0E+00	0.27	2.6E-02	5.0E-02	0.04	6.9E-04	5.0E-03	0.10	1.9E-03	6.7E-03
$WFPS_C$	0.03	-3.3E-03	2.4E-02	0.02	-1.8E-03	2.3E-02	0.01	2.9E-04	2.4E-02	0.31	-1.9E-01	3.4E-01
Site × Year	0.00	0.0E+00	0.0E+00	0.02	-2.5E-03	4.1E-02	0.06	-1.9E-02	9.5E-02	0.02	9.0E-04	2.1E-02
Site × NO_3^-	1.00	-3.7E-01	9.3E-02	0.02	-2.0E-03	3.3E-02	0.12	4.3E-02	1.4E-01	0.02	-1.2E-04	2.0E-02
Site × NH_4^-	1.00	4.0E-01	7.2E-02	0.29	1.8E-01	3.3E-01	0.05	1.7E-02	9.2E-02	0.10	1.5E-02	5.7E-02
Site × ST	1.00	6.0E-02	8.6E-03	1.00	1.8E-01	4.2E-02	0.03	-1.7E-04	1.9E-03	0.05	4.8E-04	2.9E-03
Site × $WFPS_C$	0.00	0.0E+00	0.0E+00	0.57	2.6E-01	2.6E-01	0.01	-4.6E-04	1.8E-02	0.42	-1.5E-01	2.0E-01
Year × NO_3^-	1.00	1.9E-01	4.0E-02	0.03	1.7E-03	1.7E-02	0.05	4.3E-03	3.4E-02	1.00	4.3E-01	8.4E-02
Year × NH_4^+	0.68	-1.7E-01	1.4E-01	0.01	1.0E-04	1.5E-02	0.43	-1.4E-01	2.0E-01	0.02	2.1E-04	1.4E-02
Year × ST	0.00	0.0E+00	0.0E+00	0.19	-1.8E-02	4.0E-02	0.04	-5.6E-04	3.4E-03	0.03	2.8E-04	2.3E-03
Year × $WFPS_C$	1.00	-2.3E-01	5.1E-02	0.03	-3.4E-03	3.0E-02	1.00	-4.1E-01	1.1E-01	0.92	-6.8E-01	2.7E-01
NO_3^- × NH_4^+	0.00	0.0E+00	0.0E+00	0.09	9.3E-03	4.2E-02	0.03	-1.3E-03	1.2E-02	0.02	-1.4E-04	6.3E-03
NO_3^- × ST	0.08	7.1E-04	2.7E-03	0.76	1.2E-02	7.6E-03	0.02	1.7E-05	4.6E-04	0.02	-4.2E-05	6.6E-04
NO_3^- × $WFPS_C$	1.00	9.4E-02	1.9E-02	0.01	8.2E-05	7.0E-03	0.02	4.2E-04	6.1E-03	0.03	2.0E-03	1.7E-02
NH_4^+ × ST	1.00	2.3E-02	5.6E-03	0.03	7.9E-04	6.2E-03	1.00	4.2E-02	9.5E-03	0.33	6.8E-03	1.0E-02
NH_4^+ × $WFPS_C$	0.06	3.2E-03	1.5E-02	1.00	2.4E-01	4.0E-02	0.03	-3.2E-04	1.2E-02	0.21	5.9E-02	1.3E-01
ST x $WFPS_C$	1.00	2.5E-02	3.0E-03	0.03	7.5E-05	1.4E-03	1.00	3.5E-02	4.7E-03	1.00	5.0E-02	1.1E-02

Table S2. cont.

	Soy phase			Switchgrass			Miscanthus			Poplar		
Factor	**Prob.**	**Est.**	**SE**	**Prob.**	**Est.**	**SE**	**Prob.**	**Est.**	**SE**	**Prob.**	**Est.**	**SE**
Intercept	1.00	1.5E+00	1.8E-01	1.00	2.0E+00	4.8E-01	1.00	1.1E+00	2.7E-01	1.00	1.4E+00	1.4E-01
Site	0.56	-4.4E-01	4.3E-01	0.17	-2.2E-01	5.8E-01	0.53	-7.8E-01	8.3E-01	1.00	-7.7E-01	1.5E-01
Year	0.06	-2.2E-02	1.1E-01	0.12	8.1E-02	2.5E-01	0.01	9.5E-05	1.7E-02	0.02	-2.2E-03	2.5E-02
NO_3^-	0.13	3.8E-02	1.1E-01	0.04	4.4E-03	3.1E-02	0.12	3.9E-02	1.2E-01	0.04	-2.4E-03	3.0E-02
NH_4^+	0.08	-2.2E-02	9.3E-02	0.90	-1.5E+00	5.8E-01	0.13	3.4E-02	1.1E-01	0.09	9.3E-03	5.5E-02
ST	0.07	2.4E-03	1.1E-02	0.14	7.0E-03	2.0E-02	0.23	8.2E-03	1.7E-02	0.04	7.3E-04	4.5E-03
$WFPS_C$	0.14	2.4E-02	7.4E-02	0.07	1.1E-02	1.0E-01	0.04	-5.5E-03	9.2E-02	0.02	-2.3E-03	3.4E-02
Site × Year	0.02	-4.9E-03	4.9E-02	0.02	2.5E-03	4.0E-02	0.05	1.7E-02	9.5E-02	0.01	-8.6E-04	2.3E-02
Site × NO_3^-	0.47	-4.1E-01	4.7E-01	0.96	-1.2E+00	4.6E-01	0.04	2.4E-02	1.5E-01	0.01	7.3E-05	2.1E-02
Site × NH_4^-	0.02	-1.3E-03	2.1E-02	1.00	1.1E+00	3.2E-01	0.05	-1.8E-02	1.1E-01	0.04	6.0E-03	3.7E-02
Site × ST	0.05	1.3E-03	7.4E-03	0.20	1.5E-02	3.5E-02	0.55	5.0E-02	5.1E-02	0.01	1.0E-04	2.4E-03
Site × $WFPS_C$	0.02	-1.7E-03	2.7E-02	0.05	-1.3E-02	7.1E-02	0.02	-2.2E-03	2.7E-02	0.21	-5.1E-02	1.1E-01
Year × NO_3^-	0.85	2.9E-01	1.7E-01	0.89	4.1E-01	1.9E-01	0.02	-1.3E-03	1.8E-02	0.10	-1.7E-02	6.0E-02
Year × NH_4^+	0.44	-2.0E-01	2.6E-01	0.02	-1.4E-03	3.2E-02	0.01	5.6E-04	1.9E-02	0.05	1.3E-02	6.9E-02
Year × ST	0.08	-2.6E-03	1.0E-02	0.07	1.5E-03	7.0E-03	0.02	1.7E-04	1.9E-03	0.02	-1.5E-04	1.6E-03
Year × $WFPS_C$	0.03	-2.6E-03	3.2E-02	0.02	-1.2E-03	2.8E-02	0.50	-2.2E-01	2.6E-01	0.69	-2.2E-01	1.8E-01
NO_3^- × NH_4^+	0.16	-3.7E-02	9.8E-02	0.02	2.5E-04	9.9E-03	0.08	1.2E-02	4.7E-02	0.02	-5.7E-04	8.1E-03
NO_3^- × ST	0.02	-6.0E-05	8.4E-04	0.02	7.0E-05	1.2E-03	0.86	1.9E-02	9.1E-03	0.87	1.1E-02	5.9E-03
NO_3^- × $WFPS_C$	0.13	1.6E-02	4.9E-02	0.02	7.6E-04	1.5E-02	0.75	1.2E-01	8.7E-02	0.01	1.9E-04	6.0E-03
NH_4^+ × ST	0.99	3.1E-02	9.2E-03	0.90	7.1E-02	2.8E-02	0.07	8.1E-04	3.7E-03	0.23	2.7E-03	5.9E-03
NH_4^+ × $WFPS_C$	0.06	9.2E-03	4.5E-02	0.02	-1.0E-04	1.8E-02	0.01	-4.9E-05	1.3E-02	0.03	2.8E-03	2.2E-02
ST x $WFPS_C$	0.50	6.6E-03	7.6E-03	0.96	2.5E-02	8.9E-03	0.99	3.4E-02	1.1E-02	1.00	3.8E-02	6.6E-03

Table S2. cont.

	Native grass mix			Old field			Restored prairie		
Factor	**Prob.**	**Est.**	**SE**	**Prob.**	**Est.**	**SE**	**Prob.**	**Est.**	**SE**
Intercept	1.00	9.9E-01	2.6E-01	1.00	1.1E+00	1.4E-01	1.00	6.1E-01	8.3E-02
Site	0.60	-9.6E-01	9.2E-01	0.25	-4.4E-01	8.3E-01	0.03	-1.1E-02	8.4E-02
Year	0.05	2.2E-02	1.2E-01	0.03	3.7E-03	4.8E-02	0.19	3.4E-02	8.4E-02
NO_3^-	0.54	1.2E-01	1.3E-01	0.53	2.7E-01	3.2E-01	0.12	1.0E-02	3.9E-02
NH_4^+	0.01	-6.0E-04	1.5E-02	0.04	6.3E-03	4.7E-02	0.05	6.3E-03	3.6E-02
ST	0.24	7.8E-03	1.6E-02	0.04	-5.3E-04	3.8E-03	0.01	-6.8E-06	7.8E-04
$WFPS_C$	0.12	-2.8E-02	1.6E-01	0.07	8.4E-03	3.9E-02	0.03	1.6E-03	1.4E-02
Site × Year	0.82	7.4E-01	4.3E-01	0.03	5.2E-03	6.8E-02	0.04	6.9E-03	4.1E-02
Site × NO_3^-	0.32	-2.6E-01	4.4E-01	0.78	-8.6E-01	5.3E-01	0.06	1.6E-02	8.7E-02
Site × NH_4^-	0.01	-3.2E-03	4.2E-02	0.02	4.0E-03	4.9E-02	0.18	6.4E-02	1.5E-01
Site × ST	0.61	4.4E-02	4.1E-02	1.00	8.8E-02	3.0E-02	0.03	1.1E-04	1.2E-03
Site × $WFPS_C$	0.01	6.9E-04	1.8E-02	0.38	1.4E-01	2.0E-01	0.07	-9.8E-03	4.4E-02
Year × NO_3^-	0.01	-7.1E-04	1.5E-02	0.75	2.9E-01	2.1E-01	0.04	3.3E-03	2.1E-02
Year × NH_4^+	0.08	-3.6E-02	1.5E-01	0.03	5.5E-03	4.9E-02	0.02	6.1E-04	1.3E-02
Year × ST	0.17	5.1E-03	1.2E-02	0.03	-2.8E-04	2.3E-03	0.02	6.5E-05	8.2E-04
Year × $WFPS_C$	0.05	-1.3E-02	7.2E-02	0.09	1.4E-02	5.4E-02	0.02	3.2E-04	6.8E-03
NO_3^- × NH_4^+	0.02	9.2E-04	1.7E-02	0.16	2.6E-02	7.5E-02	0.04	2.2E-03	1.4E-02
NO_3^- × ST	0.42	6.0E-03	7.9E-03	0.43	-1.4E-02	1.9E-02	0.03	-1.3E-04	1.8E-03
NO_3^- × $WFPS_C$	0.06	8.9E-03	4.0E-02	0.04	3.6E-03	2.5E-02	0.04	-2.1E-03	1.3E-02
NH_4^+ × ST	0.01	8.2E-05	1.1E-03	0.12	1.8E-03	6.0E-03	0.03	1.1E-04	9.1E-04
NH_4^+ × $WFPS_C$	0.01	1.8E-03	2.5E-02	0.02	1.8E-03	1.8E-02	0.02	1.5E-03	1.3E-02
ST x $WFPS_C$	0.95	1.9E-02	1.0E-02	0.09	6.9E-04	2.6E-03	0.03	1.3E-04	9.8E-04

Column headings are posterior inclusion probability (Prob.), based on the total likelihood of models containing that factor, estimated effect size (Est.), and standard error of Est (SE). Log transformations of NO_3^- and NH_4^+ values were used for model estimate, ST is soil temperature in °C, $WFPS_C$ is centered water filled pore space and is unitless (see text for details). Daily N_2O fluxes were measured in g N_2O-N ha^{-1} day^{-1} and inverse hyperbolic sine transformed prior to analysis, rendering the estimated effect sizes lack a consistent unit interpretation.

Table S3. Coefficients of determination between daily N_2O flux observations and predictions modeled from environmental parameters

		Model training data										
		Full data	Cont. corn	Corn phase	Canola phase	Soy phase	Switch.	Misc.	Poplar	Native mixed grass	Old field	Restored prairie
Observed data	Full data	**0.33**	0.22	0.23	0.23	0.19	0.20	0.27	0.22	0.24	0.07	0.02
	Continuous corn	0.39	**0.46**	0.36	0.23	0.20	0.21	0.32	0.25	0.30	0.02	0.01
	Corn phase	0.43	0.36	**0.48**	0.32	0.29	0.19	0.41	0.37	0.31	0.00	0.00
	Canola phase	0.23	0.12	0.13	**0.31**	0.08	0.11	0.14	0.05	0.06	0.06	0.07
	Soy phase	0.19	0.12	0.16	0.12	**0.30**	0.10	0.15	0.21	0.09	0.00	0.02
	Switchgrass	0.18	0.09	0.08	0.05	0.11	**0.27**	0.09	0.10	0.13	0.04	0.00
	Miscanthus	0.31	0.24	0.29	0.22	0.19	0.14	**0.39**	0.27	0.31	0.03	0.00
	Poplar	0.39	0.24	0.38	0.27	0.41	0.10	0.42	**0.52**	0.31	0.01	0.04
	Native grasses	0.16	0.10	0.09	0.08	0.03	0.08	0.15	0.06	**0.21**	0.11	0.01
	Old field	0.08	0.07	0.01	0.02	0.01	0.06	0.04	0.01	0.08	**0.17**	0.01
	Restored prairie	0.02	0.01	0.00	0.02	0.00	0.00	0.01	0.00	0.02	0.00	**0.06**

Predictive models were trained using either cropping system-specific subsets of data or the full dataset. Values in bold indicate R^2 values obtained during model training. Abbreviated cropping systems are continuous corn (cont. corn), switchgrass (switch.), and miscanthus (misc.).

Appendix S1. Statistical analysis details

Flux estimation and aggregation

Packages

HMR (v 0.3.1)

Flux estimation workflow

Data are organized into the data frame '`conc`':

`conc`	Dataframe containing trace gas concentrations for individual timepoints during static chamber deployment; concentration data would have undergone initial visual inspection for outliers or other chamber-associated errors
`$site`	2-level factor, study site
`$date`	Sampling date
`$trt`	10-level factor, cropping systems treatment
`$block`	9-level factor, sample block within cropping systems experiment
`$series`	String, concatenation of date, site, block, and trt fields; provides a unique identifier for a chamber sampled on a specific date while allowing for reconstruction of treatment information from HMR output (see below)
`$d.min`	Deployment time, in minutes
`$n2o`	Concentration of N_2O, in ppm
`$co2`	Concentration of CO_2, in ppm
`$ch4`	Concentration of CH_4, in ppm
`$height.m`	Static chamber headspace height, in meters
`$area.m2`	Area of soil surface within static chamber, in m^2
`$vol.m3`	Static chamber headspace volume, in m^3

The function `HMR()` requires an external file with very precise formatting, so `conc` is used to prepare the data frame '`hmr.in`':

`hmr.in`	Dataframe formatted for the HMR package and eponymous function
`$series`	`conc$series`
`$V`	`conc$vol.m3`
`$A`	`conc$area.m2`
`$Time`	`conc$d.min`
`$Concentration`	`conc$n2o`

The nonlinear HM model fits three parameters to a concentration accumulation curve, so only series with ≥4 observations are appropriate candidates for nonlinear flux estimation. The number of observations in each series is determined with the `table()` function, which is used to subset `hmr.in` into `hmr.lin` with 3 observations per series and `hmr.nlin` with ≥4 observations per series. Series with only two observations are discarded.

The dataset suitable for nonlinear flux estimation is written to a file:

```
> write.table(hmr.nlin, "hmr_input.txt", sep =";", quote=FALSE,
+ row.names=FALSE)
```

This can then be processed by `HMR()`:

```
> HMR(hmr_input.txt", FollowHMR=TRUE, LR.always=TRUE)
```

It should be noted that `HMR` version 0.4.1 introduces the argument `kappa.fixed`, which influences how the standard error of the flux is calculated. For full compatibility with this analysis, this variable should be set to `FALSE`.

Fluxes from the set of series with insufficient observations for nonlinear analysis are calculated individually for each series (`hmr.lin.subset`) by simple linear regression:

```
> lr(Concentration ~ Time, data=hmr.lin.subset)
```

The flux value will be the slope of this relationship. To match the values produced by `HMR`, these flux values must be adjusted by the effective chamber height, which is the ratio of chamber volume to soil surface area within the chamber:

```
> hmr.lin.subset$V/hmr.lin.subset$A
```

Flux values from this linear regression are then reformatted to match the output of the `HMR()` function, at which point the data can be merged. It is advisable to use the `Warning` field to note series fit with only 3 observations.

The `HMR()` function classifies fluxes as either linear, nonlinear, or no flux. The function takes nonlinear fluxes to be the baseline case, so we imposed the additional restriction of requiring that the 95% confidence interval of a nonlinear flux estimate not include the linear flux estimate for that series to be considered truly nonlinear. Once flux types are assigned to all series, there is a second round of visual inspection that reinspects the data for evidence of failed vials or other mechanical errors in light of the type of flux that was observed. If additional data are removed during this reinspection process, fluxes from those series are recalculated using the remaining data.

Once final flux estimates have been generated, it is necessary to convert fluxes from a change in mol fraction of N_2O to a change in mass N_2O-N. First, mol fraction is converted to mol flux through the Ideal Gas Law (using measured air temperature and assuming a pressure of 1 atmosphere). Then, mol flux is converted to mass flux using a mass of 28 g N per mol N_2O. At this point N_2O flux is calculated per m^2 per minute, and should be converted to flux per day with an appropriate unit of area. Note the assumption that this point measurement represents an average flux over the entire day.

Flux aggregation workflow

Annual N_2O emissions are calculated by aggregating measured daily fluxes, linearly interpolating between flux measurements, and integrating over the course of a year using trapezoidal integration. Flux data are first organized into the dataframe '`hmr.out`':

`hmr.out`	Dataframe containing N_2O flux estimates, as described above
`$site`	2-level factor, study site
`$date`	Sampling date
`$trt`	10-level factor, cropping systems treatment
`$block`	9-level factor, sample block within cropping systems experiment
`$year`	3-level factor, year when sample was taken
`$n2o.ha.day`	N_2O flux, in g N_2O-N ha^{-1} day^{-1}

A subset of this dataframe, `hmr.sub`, is created for each unique combination of `trt`, `block`, and `year`. This subset contains all flux measurements taken from a given plot in one year, which will be used to estimate aggregate emissions from that year. As described in the text, we assume that frozen soils (10 cm temperature < 0 °C) do not emit N_2O. From this assumption, we define `last.fro` and `first.fro` as the last date in the spring and first day in the fall, respectively, to have frozen soils. The endpoints of the N_2O emission period for a year are thus defined as:

```
> strt.date <- min(last.fro, min(hmr.sub$date))
> stop.date <- max(first.fro, max(hmr.sub$date))
```

Using these dates, we generate the vector '`dates`' which contains all dates for which we have flux data and the endpoints of the emissions period, and the vector '`fluxes`' which contains observed fluxes and the assumed 0 flux for the endpoints:

```
> dates <- c(strt.date, hmr.sub$date, stop.date)
> fluxes <- c(0, hmr.sub$n2o.ha.day, 0)
> n.obs <- length(dates)
```

Note that when flux measurements were taken after the emission period endpoints, the dates of those measurements are instead used as endpoints. Trapezoidal integration is then used to calculate a single flux over the entire year:

```
> d.dates <- dates[2:n.obs] – dates[1:(n.obs-1)]
> m.fluxes <- (fluxes[2:n.obs] + fluxes[1:(n.obs-1)])/2
> d.dates %*% m.fluxes
```

Statistical analysis of annual emissions

Packages

`AICcmodavg` (v 2.0-3)
`lsmeans` (v 2.15)
`nlme` (v 3.1)
`plyr` (v 1.8.1)

Analysis of summed 3-year annual emissions

Cumulative aggregate emissions were summed within each plot to produce the data table 'n2o.sum':

`n2o.sum`	Dataframe containing cumulative N_2O emissions from plots in the experiment
`$site`	2-level factor, study site
`$trt`	10-level factor, cropping systems treatment (note that for the corn-soy-canola rotational systems, this factor refers to a specific rotation, with all of its phases; given the duration of this study, each phase is represented exactly once)
`$levels`	20-level factor, all unique combinations of site and trt, for use with factor level collapse
`$block`	9-level factor, sample block within cropping systems experiment
`$plot`	90-level factor, individual field plot
`$flux`	3-year summed N_2O emissions, g N_2O-N ha^{-1}

Cumulative fluxes are log-transformed, and a mixed-effects model is used to analyze site and cropping system differences, with block as a random effect:

```
> sum.lme.0 <- lme(log(flux.sum) ~ site * trt, random = ~1|block,
+ data = n2o.sum)
```

Variance is allowed to differ among levels of site, trt, or both, and the models with the lowest BIC value is used:

```
> sum.lme.1 <- update(sum.lme.0, weights = varIdent(form = ~1|site))
> sum.lme.2 <- update(sum.lme.0, weights = varIdent(form = ~1|trt))
> sum.lme.3 <- update(sum.lme.0,
+ weights = varIdent(form = ~1|site * trt))
> anova(sum.lme.0, sum.lme.1, sum.lme.2, sum.lme.3)
```

```
          Model df    AIC    BIC  logLik   Test  L.Ratio  p-value
sum.lme.0     1 22 169.50 218.33  -62.75
sum.lme.1     2 23 167.13 218.18  -60.58  1 vs 2  4.36216  0.0367
sum.lme.2     3 31 172.88 241.69  -55.44  2 vs 3 10.24999  0.2479
sum.lme.3     4 41 170.02 261.02  -44.01  3 vs 4 22.86445  0.0113
```

As shown above, our data are most parsimonious with variances that differ by site, but not among treatments (`sum.lme.1`). Using this as our baseline model, we then identify significantly different `site` × `trt` groups by factor level collapse. The model is first updated, using a single factor with a level for each unique treatment:

```
> sum.lme.F <- update(sum.lme.1, ~ levels)
```

Starting from this model, factor level collapse is an iterative process consisting of three steps.

Step 1: Identify most similar clusters using the Z ratio of their LS means

```
> sum.lsm.F <- lsmeans(sum.lme.F, pairwise ~ levels,
+ data=sum.lme.F$data)[[2]]
> arrange(summary(sum.lsm.F), abs(z.ratio))

contrast     estimate        SE df     z.ratio  p.value
L2 - L8   0.001546928 0.3411971 NA  0.004533824  1.0000
L6 - L14 -0.016234264 0.3242299 NA -0.050070217  1.0000
L9 - L15 -0.022193434 0.3242299 NA -0.068449673  1.0000
...
```

Step 2: Recode the levels term to merge the two most similar levels and update the model

```
> n2o.sum$levels.1 <- n2o.sum$levels
> levels(n2o.sum$levels.1)[c(2,8)] <- "L2,8"
> sum.lme.1 <- update(sum.lme.F, ~ levels.1)
```

Step 3: Compare the second-order AIC of the new and previous model

```
> AICc(sum.lme.F) > AICc(sum.lme.1)
```

If the AICc of the newer model is smaller than that of the prior model, indicating a more parsimonious representation of the data, start the process again from step 1, using the newer model as the starting point. Using this approach, treatments will iteratively be clustered into groups that can be modeled as having the same mean without substantively impacting the model's fit to the data. Once the two most similar groups cannot be joined without increasing AICc, the groups present in the prior model are assumed to be significantly distinct from each other. The outcome of this analysis was used to generate Figure 1 in the manuscript.

Analysis of annual aggregate emissions

We analyzed annual aggregate emissions separately for each site-year. Otherwise, these data were analyzed in the same fashion as the emissions summed over three years with regards to model building and factor level collapse. The outcome of this analysis was used to generate Figure 2 in the manuscript.

Estimation of daily fluxes with Bayesian Model Averaging

Packages

`BMA` (v 3.16.2.2)

Model building

Bayesian Model Averaging begins with the data frame 'bma.in':

`bma.in`	Dataframe containing daily N_2O flux estimates for which we also have data on soil parameters hypothesized to influence N_2O production
`$year`	2-level factor, sampling year; 2009 was excluded from this analysis because a different method was used for measuring NO_3^- and NH_4^+
`$site`	2-level factor, study siteg
`$system`	10-level factor, cropping system; differs from trt in that rotations are grouped by phase (e.g. corn, soy, canola), rather than by specific ordering as before
`$n2o.ha.day`	N_2O flux, in g N_2O-N ha^{-1} day^{-1}
`$log.nh4`	Log-transformed soil NH_4^+ concentration, with a floor of half of the smallest positive concentration
`$log.no3`	Log-transformed soil NO_3^- concentration, with a floor of half of the smallest positive concentration
`$soil.t`	Soil temperature, °C
`$wfps.c`	Water-filled pore space, scaled and centered by site

We then use the `bic.glm()` function to evaluate the set of all explanatory variables and their second-order interactions as predictors of N_2O flux. Site and year are included as predictors to allow for different responses to soil parameters under distinct conditions. Note that fluxes are hyperbolic arcsine-transformed. This was done to approximate log transformation of these values while retaining negative fluxes.

```
> form <- formula(asinh(n2o.ha.day) ~ (site + year + log.no3 +
+ log.nh4 + soil.t + wfps.c)^2)
> full.bma <- bic.glm(form, data=bma.in, glm.family="Gaussian",
+ maxCol=100, occam.window=TRUE)
```

This model can then be used to predict N_2O fluxes for a given set of environmental conditions. This version of `BMA` creates idiosyncratic labels for factors, so these must be renamed to be compatible with the `predict()` function.

```
> colnames(full.bma$mle)[c(2,3,8)] <- c("siteKBS", "year2011",
+ "siteKBS:year2011")
> predict(full.bma, bma.in)
```

While this approach used the entire dataset to both train and evaluate the model, we also trained models from subsets of the data corresponding to specific systems (e.g. switchgrass):

```
> switch.in <- subset(bma.in, system == “switchgrass”)
> switch.bma <- bic.glm(form, data=switch.in, glm.family=”Gaussian”,
+ maxCol=100, occam.window=TRUE)
> colnames(switch.bma$mle)[c(2,3,8)] <- c(“siteKBS”, “year2011”,
+ “siteKBS:year2011”)
> predict(switch.bma, bma.in)
```

At this point, the model based on the relationships among soil parameters and N_2O fluxes in switchgrass is used to predict N_2O fluxes based on the soil parameters found in other systems. The outcomes of this process were used to generate Figure 4 and Table 2.